DOI: 10.18462/iir.nh3-co2.2023.0035

Investigation of CO_2 refrigeration system and thermal energy storage for passenger ships

Henrik ANDERSEN[(a)], Muhammad Zahid SAEED[(a)], Armin HAFNER[(a)], Cecilia H. GABRIELII[(b)]

(a) Norwegian University of Science and Technology
Trondheim, 7491, Norway, muhammad.z.saeed@ntnu.no
(b) SINTEF Energy Research
Trondheim, 7491, Norway, cecilia.gabrielii@sintef.no

ABSTRACT

As dominant synthetic refrigerants are increasingly regulated, natural refrigerants have been resurrected as working fluids. Like all other sectors, the cruise industry must adapt to reduce GHG emissions. More emphasis has been given to natural working fluids, such as water, ammonia, hydrocarbons, and carbon dioxide, than new synthetic refrigerants. Among the natural refrigerants, CO_2 refrigerant is the only non-toxic and non-flammable and offers compact units suited for cruise ships. Cruise ships utilise refrigeration systems for air-conditioning and to preserve provision. The performance of two CO_2 refrigeration systems employed for air conditioning and provision chilling and freezing aboard a medium-sized cruise ship is simulated. Furthermore, how cold thermal energy storage (CTES) can be utilised to supply the cooling demand of a two-hour port stay has been investigated. Three reference cases with different boundary conditions are defined and referred to as warm-, medium, and cold cases. Respectively for the cases, it has been found that the maximum cooling COP of an AC system is about 2.89, 4.19, and 5.99. Furthermore, for the provision system, it is 2.33, 2.98, and 3.54, respectively. Lastly, the CTES must contain 21163 kg of water as phase change material and a total volume of 38.0 m^3.

Keywords: Refrigeration, Carbon Dioxide, Transcritical, cruise ships, Thermal Energy Storage, Ejectors, Energy Efficiency.

1. INTRODUCTION

Tourism provides people with delight and relaxation while providing economic possibilities to communities. Tourists travel by different means of transport, i.e., land-based, maritime and aviation transport. There are greenhouse emissions (GHG) associated with these means of transport. According to Grythe et al., 2021, cruises and ferries in 2018 accounted for 21% of the CO_2 emissions of Norway's tourism-related transport. However, burning fossil fuels is not the only source of GHG emissions. Nowadays, R134a, R404A and R407C are the dominating refrigerants on passenger ships, and they have a global warming potential (GWP) of 1430 or greater (Hafner et al.,2019). Leakages of such synthetic refrigerants contribute significantly to GHG emissions. Therefore, in 2014, the EU introduced the F-Gas Regulation (EU 517/2014) for fluorinated greenhouse gases Here, there is a ban for centralised refrigeration systems exceeding 40 kW capacity, relying on fluorinated greenhouse gases with a GWP of 150 or more. As an alternative refrigerant, CO_2 is a great option, as refrigeration systems utilising CO_2 have proven to be environmentally friendly, personal safe and energy efficient. Another measure towards zero emissions will require ships to connect to onshore power during port stays longer than two hours or another zero-emission technology from January 2030 (Jacobs Karin, 2022). As the port stays less than two hours will not regulate. It is interesting to investigate if cold thermal energy storage (CTES) can be utilised to cover the cooling demand during these port stays.

The aim of this work is to develop energy-efficient CO_2 refrigeration models in Dymola and simulate them to find the expected performances from such systems when applied to cruise ships. Furthermore, examine how CTES can be utilised to supply the cooling demand related to a two-hour long port stay. Since only refrigeration systems are investigated, the scope only contains summer conditions.

Author Accepted Manuscript version of the paper by Henrik Andersen et al.
in 10th IIR Conference on Ammonia and CO2 Refrigeration Technologies (2023)
DOI: http://dx.doi.org/10.18462/iir.nh3-co2.2023.0035

2. REFERENCE CASE

To conclude the system's applicability and performance, it should be applied to specific scenarios. Further, the scenarios should be representative of real applications. Furthermore, this section defines three cases containing three different cooling loads to investigate how AC- and provision system performance changes with environmental conditions.

2.1. Air conditioning and cold thermal energy storage

To the author's knowledge, very few studies exist on passenger ships' AC cooling demand. Thus, the reference cases are based on two studies, Ancona et al.2018 and Boertz et al.2020.
Boertz et al.2020 calculated the energy demand of a 139 m long and 22 m wide fuel cell-driven expedition cruise ship during constant sailing. The hottest investigated climate was with weather data collected from Singapore. The resulting cooling demand curve is shown as the red curve in Figure 1. This reference case is referred to as the warm reference case. In this case, the AC system will have to operate as a heat sink with a seawater temperature of 30 °C.
Furthermore, Boertz et al.2020 have calculated the cooling demand with weather data from Amsterdam during summer. However, these conditions are very similar to the conditions of the cold reference case defined below. Although the cooling demand was calculated for Amsterdam's climate, the profile is fairly like the Singapore case.

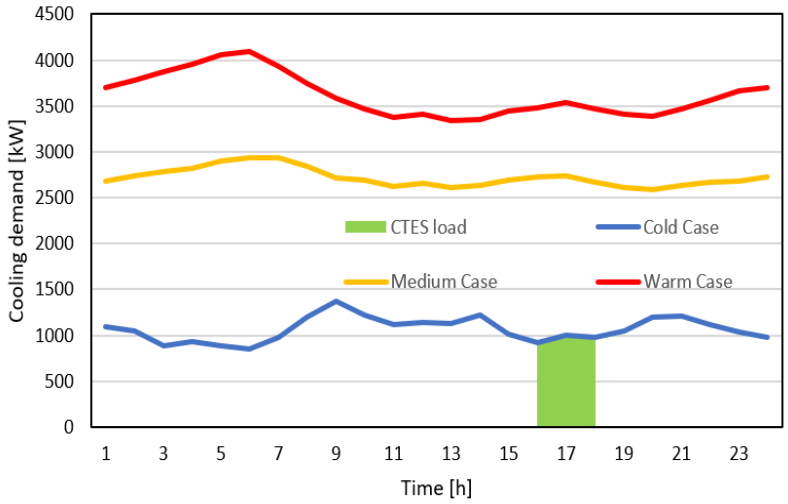

Figure 1: The cooling load for every AC reference case and the CTES load. Value for the warm- and medium case are collected from Boretz et al.2020, values for the cold case and CTES are collected from Ancona et al.2018

Therefore, the demand was linearly interpolated based on weather data collected from Barcelona during summer to get a case in between. The resulting cooling demand curve is shown in Figure 1 as the yellow curve. This reference case is referred to as the medium reference case. In this case, the AC system will have to operate with a seawater temperature of 23 °C as a heat sink. Ancona et al.2018 studied a 177 m long and 28 m wide passenger ship sailing between Stockholm and Mariehavn in Sweden. As a part of the study, energy demand was gathered through measurement and calculation. The cooling demand of the ship during summer is shown as the cold case in Figure 1. The ship makes the same route every day. The ship leaves Stockholm around 06:00 PM; after reaching the open sea, it stops for some hours prior to reaching Mariehavn early in the morning. It leaves again one hour later and arrives back in Stockholm at 04:00 PM. This reference case is referred to as the cold reference case. In this case, the AC system will have to operate with a seawater temperature of 16 °C as a heat sink.
Since the cold reference case includes port stays, it is convenient to collect data for the CTES case from here. The ship has two port stays one hour in the morning and two hours in the afternoon. From the cooling demand of the second port stay, it can be found that the CTES will have to supply 1914 kWh of cold. Fig 1 shows the cooling demand that must be supplied by the CTES, represented by the green shaded area.

Author Accepted Manuscript version of the paper by Henrik Andersen et al.
in 10th IIR Conference on Ammonia and CO2 Refrigeration Technologies (2023)
DOI: http://dx.doi.org/10.18462/iir.nh3-co2.2023.0035

2.1.1. Provision cooling and freezing

It is assumed that the ship would need a food capacity equivalent to a medium-sized supermarket. Additionally, it is assumed that the activity is low and that the provision is already chilled/frozen when stored, i.e., loading and unloading do not influence the cooling and freezing demand. It is also assumed that the construction and placement of cabinets and rooms result in constant heat leakage, i.e., the constant cooling and freezing demand. The cooling and freezing demand were collected from Tosato et al.2020, where a medium-sized supermarket was studied. Hence 90 kW of cooling and 22 kW of freezing is demanded. The system will operate under the same environmental conditions as the AC system. As a result, three cases with the same load and different heat sink temperatures were created. The key values for each case are listed in Table 1.

Table 1: Key values for the three different cases for the provision system. Cooling- and freezing load collected from [8]

Reference Case		Cold	Medium	Warm
Sea water temperature	**°C**	**16**	**23**	**30**
Cooling load	**kW**	**90**	**90**	**90**
Freezing load	**kW**	**22**	**22**	**22**

3. SYSTEM DESIGN AND SIMULATIONS

3.1. AC- and provision system

The investigated AC system is an ejector-supported two-stage evaporation system and is shown in Fig 2. From the compressor, the refrigerant enters the first of two gas coolers dedicated to heat recovery. Depending on the heat recovery demand, the gas cooler may be fully or partially bypassed through a three-way valve. The rest of the heat is rejected in the last gas cooler to seawater. The cooled-down refrigerant enters an IHX. Here, it is subcooled by the refrigerant upstream from the compressor. For work recovery purposes, the expansion device is an ejector. The expansion of the high-pressure fluid conveys the refrigerant from the secondary side (suction flow). The discharged flow enters the first evaporator before it is discharged into the liquid receiver. From here, the liquid is throttled by an expansion valve, which corresponds to the ejector pressure lift.
Further, the fluid enters the second evaporator before the ejector conveys it. The refrigerant is fully evaporated in the second evaporator prior to suction. The vapour from the liquid receiver enters the IHX, where it is superheated before the compressor compresses it. A three-way valve is installed to be able to control the superheat of the compressor suction flow. The system chills water from 12°C to 6°C before it is supplied to the HVAC system.

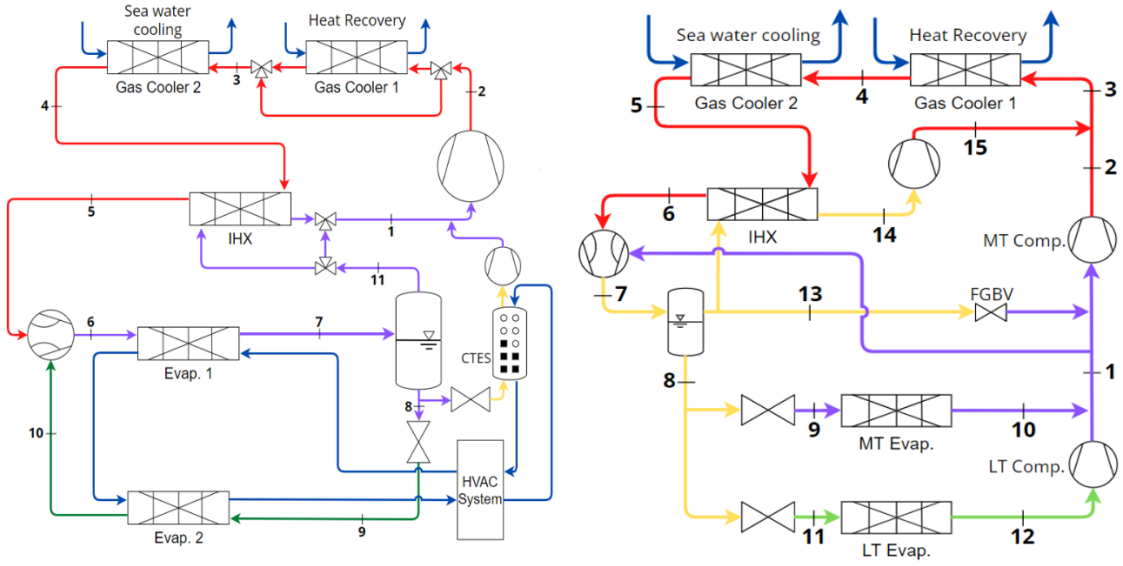

Figure 2: Simplified schematics of the AC system equipped with CTES (left) and the provision system (right)

Author Accepted Manuscript version of the paper by Henrik Andersen et al.
in 10th IIR Conference on Ammonia and CO2 Refrigeration Technologies (2023)
DOI: http://dx.doi.org/10.18462/iir.nh3-co2.2023.0035

The designed provision system is shown in Figure 2 and is an ejector-supported parallel compression system. From the MT compressor, the refrigerant enters gas cooler 1 for heat recovery. Heat is recovered by cooling water. The rest of the heat rejection happens in gas cooler 2, which utilises seawater. Further, the refrigerant passes through the IHX, which is cooled further before entering the ejector. The ejector conveys refrigerant from the suction line of the MT compressor. The mixed fluid is discharged into a liquid receiver. Since the system supplies cold to both cooling and freezing of provision, it has two evaporators fed with liquid from the receiver. The pressure in the LT evaporator is lower than in the MT evaporator. Hence this refrigerant enters the LT compressor before it is mixed with the refrigerant from the MT evaporator. The parallel compressor draws the vapour in the liquid receiver through the IHX before it is compressed to high-side pressure. Due to the ejector, increasing gas cooler pressure shifts compressor work from the MT compressor to the parallel compressor. Therefore, the MT compressor is not needed in warm climates if the receiver pressure is sufficiently low. Table 2 summarises the most important conditions of the AC- and provision system.

Table 2: Key conditions and parameters for the AC and provision system.

System AC Provision			
Temperature difference gas cooler outlet	**°C**	**5**	**5**
Receiver pressure	**bar**	**39**	**40**
MT-/first evaporator pressure	**bar**	**39**	**31.3**
LT-/second evaporator pressure	**bar**	**35**	**14.3**
Ejector efficiency	**-**	**0.3**	**0.3**
Heat recovery exit temperature	**°C**	**45**	**45**
Heat recovery gas cooler heat transfer area	**m^2**	**24.7**	**1483.6**

3.1.1. Control of high-side pressure

To control the high-side pressure of the simulated models, the second gas cooler heat transfer area is varied. High-side pressure depends on the gas cooler heat transfer area and the expansion valve or ejector needle opening. Thus, it can be changed to influence the pressure. To better see the impact on recovered heat with increasing high side pressure, the areas of the first gas coolers were not changed but fixed to the values shown in Table 2. Hence, only the heat transfer area of the second gas cooler was varied.

3.2. Cold thermal energy storage

The CTES utilises latent heat storage with water as phase change material (PCM). It must be able to be charged during sailing and discharged in port. The AC system will do the charging, and the discharging is done by circulating water connected to the HVAC system. As space on board a cruise ship is limited, the final system will contain several CTES systems in parallel. Since the PCM is stored in containers, the designed systems will utilise double bundle containers.

Table 3: Key values CTES.

CTES	Unit	Size
Volume	**m^3**	**6.9**
Number of serial charging tubes	**-**	**100**
Number of parallel charging tubes	**-**	**100**
Number of parallel charging tube side flows	**-**	**100**
Number of serial discharging tubes	**-**	**42**
Number of parallel discharging tubes	**-**	**42**
Number of parallel discharging tube side flows	**-**	**42**
Total mass PCM	**kg**	**4633**

To investigate what impact CTES charging has on the AC system performance, the AC system is further developed. Figure 2 shows how the AC system configuration is equipped with CTES. When charging is initiated, liquid from the receiver is throttled to 31 bar before entering the LHS, where it is superheated at 5°C. Downstream the refrigerant is compressed to receiver pressure before being mixed with the refrigerant from

Author Accepted Manuscript version of the paper by Henrik Andersen et al.
in 10th IIR Conference on Ammonia and CO2 Refrigeration Technologies (2023)
DOI: http://dx.doi.org/10.18462/iir.nh3-co2.2023.0035

the IHX. This figure only shows how one LHS is integrated. With multiple, they would have been connected in parallel. Figure 2 also illustrates how the CTES can be discharged. Water from the HVAC system is chilled in the LHS and returned. Table 3 summarises the key values of one investigated CTES module.

4. RESULTS AND DISCUSSIONS

4.1. AC system performance

The graphs in Figure 3 show the dynamic performance of the modelled AC system. The $COP_{c,AC}$ curves represent the best obtainable performance from the simulated system during each case. During the warm case, the system operates with a $COP_{c,AC}$ in the range of 2.863-2.867. Further, in the medium case, it is able to operate in the range of 4.185-4.188. Moreover, finally, in the coldest case, the $COP_{c,AC}$ is in the range of 5.982-6.000. The medium and cold cases have not yet converged during the first hours. Thus, values from here are unreliable.

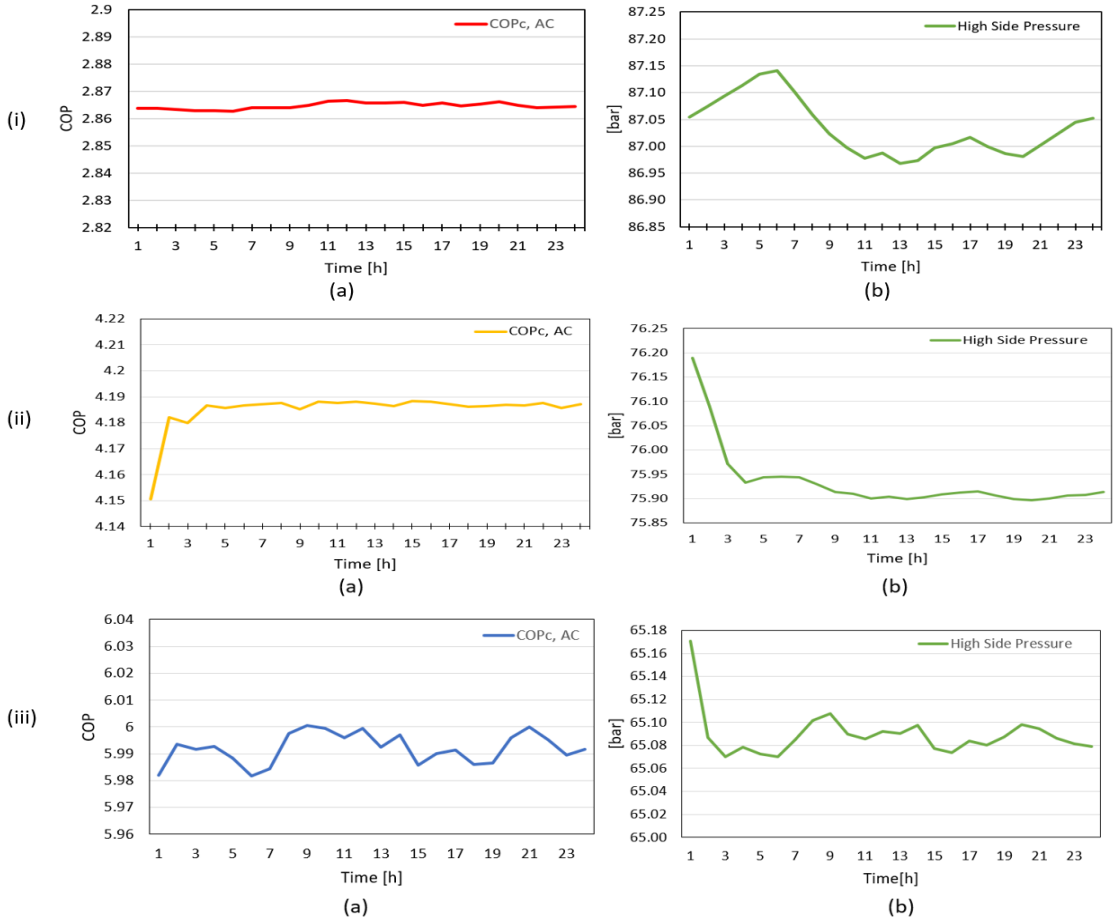

Figure 3: AC system dynamic performance for each case. (i), (ii) and (iii) represents to the warm, medium and cold case, respectively. (a) illustrates the $COP_{c,AC}$ and (b) the corresponding high side pressure.

As expected, the high side pressures increase with increasing cooling load. Further, it was expected that the lowest COPc, AC, would occur with the highest pressures and vice versa. This trend can only be seen in the warm case. Unexpectedly, this is not the situation for the two other cases. As a matter of fact, in the coldest case, the highest COPc, AC occurs with the highest pressures. However, if the high side pressure is increased, the $COPc_{,AC}$ fluctuations behave as expected, so the behaviour is most likely due to instabilities in the control system and small state changes in other parts of the system.

Because of two-staged evaporation, both the low side pressure and the receiver pressure have to be fixed. So, by bypassing the ejector with a proportion of the refrigerant through a valve, the system is able to control the pressure lift generated by the ejector, thus, the pressure levels in the heat exchangers. Because of this, it would have been interesting to compare the AC system with an ejector-supported one-staged evaporator system. When having only one evaporator pressure, the receiver pressure may fluctuate. Thus, all of the pre-

Author Accepted Manuscript version of the paper by Henrik Andersen et al.
in 10th IIR Conference on Ammonia and CO2 Refrigeration Technologies (2023)
DOI: http://dx.doi.org/10.18462/iir.nh3-co2.2023.0035

compression capacity of the ejector can be utilised. On the other hand, the employment of one-staged evaporation would increase the exergy destruction rate.

4.2. Provision system performance

From Table 4, the provision system performance can be seen. As for the AC system, the listed $COP_{c,prov}$ is the highest obtainable system performance for each case. As expected the $COP_{c,prov}$ greatest for the coldest case and least for the warm case. This is, of course, due to the heat sink temperature being greatest for the warm case and least for the cold state. The high-side pressure also reflects this. The difference in heat sink temperature also influences the work allocation between the compressors. The LT compressor work is the same for all cases, but one can see that work is shifted from the MT compressor to the parallel compressor with increasing heat sink temperature. Due to the increase in gas cooler exit temperature and the increase in ejector entertainment ratio, more work has to be done by the parallel compressor and less is required by the MT compressor.

Table 4: Provision system performance and key numbers.

Reference case	Unit	Warm	Medium	Cold
$COP_{c,\ prov}$	-	2.334	2.997	3.538
High side pressure	bar	86	76	70
Gas cooler outlet temperature	°C	35	28	21
Parallel compressor work	kW	28.45	12.98	6.18
MT compressor work	kW	14.86	20.02	20.80
LT compressor work	kW	4.67	4.67	4.67
Entrainment ratio	-	0.31	0.20	0.13

4.3. Heat recovery and optimum high side pressure

In this section, the possibility of heat recovery is presented. Since the first gas cooler in both systems is dedicated to heat recovery, increasing high side pressure will shift heat rejection from the second to the first gas cooler. At the same time, the optimum high side pressure for each system is investigated. Hence, it is presented together.

4.3.1. Heat recovery and optimum high-side pressure for the AC system

Since the AC system is simulated with a dynamic cooling load, the $COP_{c,AC}$ fluctuate, as shown above. Therefore, the values in this section are collected from where the system supplies the maximum cooling load. Figure 4 shows the heat recovery and optimum high side pressure for the AC system during the warm case. In (a), it can be seen that with regards to $COP_{c,\ AC}$, the optimum high side pressure is 87 bar. Further, the reduction in $COP_{c,AC}$ with increasing pressure is relatively small. As expected, does the $COP_{rec,AC}$ increase with increasing high side pressure before it reaches a maximum of approximately 3.2.

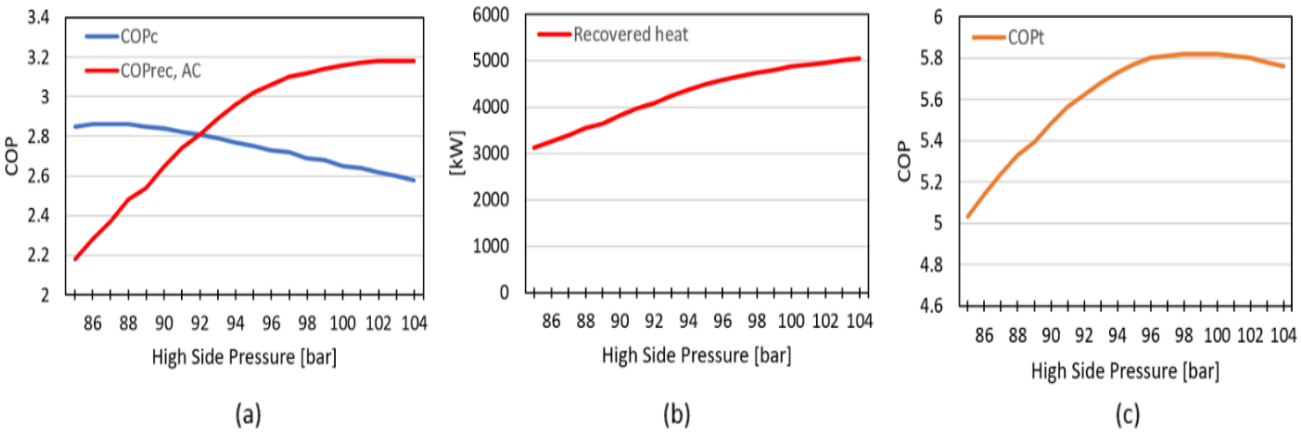

Figure 4: Heat recovery and optimum high side pressure for the AC system during the warm case. With increasing high side pressure: (a) the change in COP_c and $COP_{rec,\ AC}$; (b) the change in total amount of heat recovered; (c) the change in COP_t. Gas cooler outlet temperature = 35°C.

Author Accepted Manuscript version of the paper by Henrik Andersen et al.
in 10th IIR Conference on Ammonia and CO2 Refrigeration Technologies (2023)
DOI: http://dx.doi.org/10.18462/iir.nh3-co2.2023.0035

In (b), the total recovered heat is shown. The investigated high side pressures allow the system to recover between 3000 kW and 5000 kW heat. In (c), the $COP_{t,AC}$ is shown. It reaches a maximum at approximately 99 bar. From here, increasing high side pressure will result in decreasing $COP_{t,AC}$. In other words, if the pressure is increased more, the payback of cold and heat is less than the electricity required to drive the compressor. As for the warm case, the $COP_{c,\ AC}$ in the medium- and cold case decreases with increasing high side pressures. However, due to the relatively low gas cooler outlet temperature, they do not have an optimum high side pressure with regards to $COP_{c,\ AC.}$ Further, the smallest amount of heat recovered occurs at the lowest pressure in the cold case. At that point, the system is able to recover 400 kW of heat.

4.3.2. Heat recovery and optimum high-side pressure for the provision system

Figure 5 illustrates the results from investigating heat recovery and optimum high side pressure for the provision system during the warm case. The $COP_{c\ prov}$ is depicted in (a). In contrast to the AC system, the provision system is not able to reach a maximum, even with the relatively high gas cooler outlet temperature. This is because the model is not able to reduce the pressure below 86 bar. In parallel, the $COP_{rec,\ prov}$ strictly increases, it does not reach a maximum either but starts to flatten out at the highest pressures. The heat recovery gas cooler in the provision system is relatively small compared to the one in the AC system, therefore the relatively small heat transfer area cause the curve to flatten out slower and later. Further, is the heat recovered depicted in (b). The system is able to recover between 90 kW and 140 kW of heat, depending on the high side pressure. Obviously, it can recover more heat by increasing the pressure further, but as shown in (c) the maximum $COPt_{,prov}$ located at approximately 103 bar.

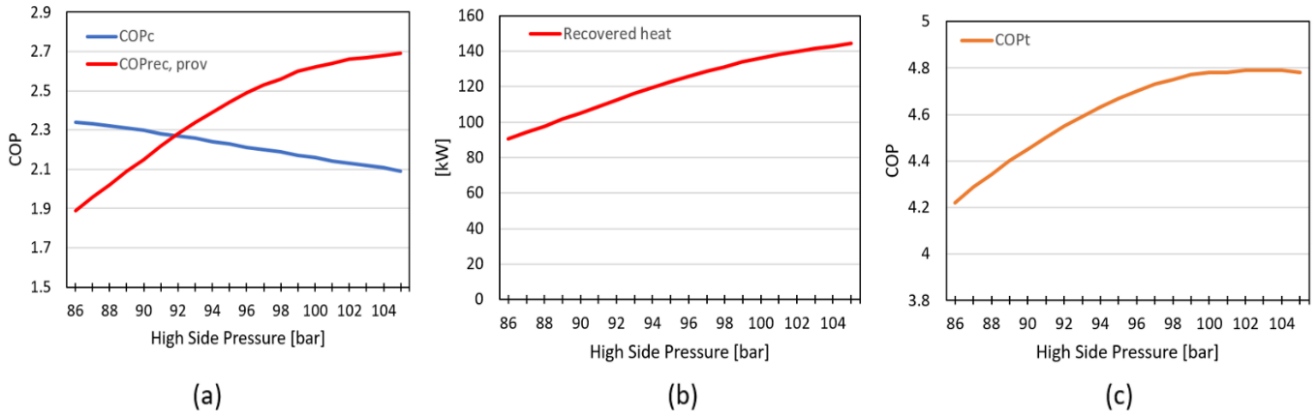

Figure 5: Heat recovery and optimum high side pressure for the provision system during the warm case. With increasing high side pressure: (a) the change in COP_c and $COP_{rec,\ prov}$; (b) the change in total amount of heat recovered; (c) the change in COP_t. Gas cooler outlet temperature = 35°C.

4.4. Cold thermal energy storage

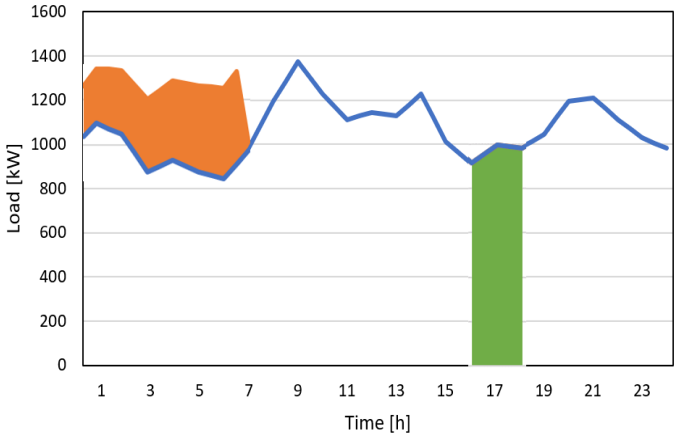

Figure 6: CTES charging strategy, CTES discharging and overall cooling load. Charging is shown as the orange shaded area and discharging as green

Several CTES modules will have to operate in parallel to meet the total cooling demand. From the simulated results, the total system will have to include 21163 kg of water as PCM and a total volume of 38.0 m^3. This translates to 4.56 parallel modules of the one specified in Table 3. Figure 6 shows a possible CTES charging strategy when all of the modules are charged at the same time. Apart from being discharged during the two-hour port stay, the system can be charged in six hours without increasing the peak load of the overall AC cooling load. During charging the $COP_{c,AC}$ is decreased in the range from 6.13% to 9.73%.

5. CONCLUSIONS

In this work, the performance of two energy-efficient CO_2 refrigeration systems for a medium-sized cruise ship, utilised for air conditioning and provision cooling and freezing, have been examined through simulation. Three reference cases with different boundary conditions were defined with corresponding cooling loads to obtain realistic results for cruise ship applications. They were referred to as the warm-, medium- and cold cases. As the AC system supplies a dynamic cooling load, the cooling COP ($COP_{c,\,AC}$) fluctuates. At the best operating point, it has been found that the high side pressure fluctuations are very small, and that the system is able to operate with a $COP_{c,\,AC}$ around 2.86, 4.19 and 5.99, respectively, for the warm-, medium- and cold cases. Next, at the best operation point, the provision system is able to operate at a $COP_{c,\,prov}$ of 2.33, 2.98 and 3.54, respectively, for the warm-, medium-, and cold cases. The AC system can recover from 400 kW to 5000 kW of heat within the three reference cases. The provision system can recover from 55 kW to 140 kW of heat. CTES have also been examined. It has been found that the CTES must contain 21163kg of water as phase change material, and a total volume of 38.0m^3, to be able to supply the cooling demand of a two-hour port stay.

ACKNOWLEDGEMENTS

The authors gratefully acknowledge the Research Council of Norway for the financial support for carrying out the present research [NFR Project No. 308779 CruiZE].

REFERENCES

Grythe, H., Aparicio, S.L.,2021. The who, why and where of Norway's CO2 emissions from tourist travel. Environmental Advances 5,100104.

Hafner, A., Gabrielii, C.H., Widell, K.N.,2019. Refrigeration units in marine vessels: Alternatives to HCFCs and high GWP HFCs. Nordic Council of Ministers.

European Commission. 2015 EU legislation to control F-gases. https://climate.ec.europa.eu/eu-action/fluorinated-greenhouse-gases/eu-legislation-control-f-gases_en

Jacobs, K.,2022. European ports becoming 'fit for 55'. EPRS, European Parliamentary Research service. https://www.europarl.europa.eu/RegData/etudes/ATAG/2022/729395/EPRS_ATA(2022)729395_EN.pdf

Ancona, M. A., Baldi, F., Bianchi, M., Branchini, L., Melino, F., Peretto, A., Rosati, J., 2018. Efficiency improvement on a cruise ship: Load allocation optimisation. Energy Conversion and Management, 164:42–58, 2018.

Boertz, C., 2020. Energy demand of a fuel cell-driven cruise ship: Analysis and improved prediction method of the operational power variation under different loading and environmental conditions. http://resolver.tudelft.nl/uuid:1526765e-8491-4576-910d-1c0f38d15b53

Tosato, G., Minetto, S., Rossetti, A., Hafner, A., Schlemminger, C., Girotto, S., 2020. Field data of co2 integrated refrigeration, heating and cooling systems for supermarkets. In Proceedings of the 14th IIR-Gustav Lorentzen Conference on Natural Refrigerants.